Stem Cell Reports
Report
OPEN ACCESS

The Spindle Assembly Checkpoint Is Required for Hematopoietic Progenitor Cell Engraftment

Andreas Brown,[1] Johannes Pospiech,[1] Karina Eiwen,[1] Darren J. Baker,[2] Bettina Moehrle,[1] Vadim Sakk,[1] Kalpana Nattamai,[3] Mona Vogel,[1] Ani Grigoryan,[1] and Hartmut Geiger[1,3,*]
[1]Institute of Molecular Medicine, Ulm University, Ulm 89081, Germany
[2]Department of Pediatric and Adolescent Medicine, Mayo Clinic, 200 First Street SW, Rochester, MN, USA
[3]Division of Experimental Hematology and Cancer Biology, Cincinnati Children's Hospital Medical Center and University of Cincinnati, Cincinnati, OH, USA
*Correspondence: hartmut.geiger@uni-ulm.de
https://doi.org/10.1016/j.stemcr.2017.09.017

SUMMARY

The spindle assembly checkpoint plays a pivotal role in preventing aneuploidy and transformation. Many studies demonstrate impairment of this checkpoint in cancer cells. While leukemia is frequently driven by transformed hematopoietic stem and progenitor cells (HSPCs), the biology of the spindle assembly checkpoint in such primary cells is not very well understood. Here, we reveal that the checkpoint is fully functional in murine progenitor cells and, to a lesser extent, in hematopoietic stem cells. We show that HSPCs arrest at prometaphase and induce p53-dependent apoptosis upon prolonged treatment with anti-mitotic drugs. Moreover, the checkpoint can be chemically and genetically abrogated, leading to premature exit from mitosis, subsequent enforced G1 arrest, and enhanced levels of chromosomal damage. We finally demonstrate that, upon checkpoint abrogation in HSPCs, hematopoiesis is impaired, manifested by loss of differentiation potential and engraftment ability, indicating a critical role of this checkpoint in HSPCs and hematopoiesis.

INTRODUCTION

Hematopoietic stem cells (HSCs) undergo self-renewal and differentiation to ultimately provide all cells of the blood system. They mostly sustain a quiescent state in the G0 phase of the cell cycle *in vivo* during which cellular and metabolic activities are held to a minimum level. Upon activation, HSCs enter the cell cycle to initiate self-renewal or differentiation. However, every round of DNA replication, due to increased metabolism and proliferation, might be associated with the generation of DNA lesions (Walter et al., 2015). Most of the time DNA damage is detected and efficiently repaired. Lesions that remain unresolved, however, might be converted into and thus fixed in the genome as mutations or chromosomal aberrations such as translocations. This might result in the deregulation of HSCs and ultimately their leukemic transformation (Holyoake et al., 1999).

As HSCs are mostly situated in the G0 state of the cell cycle, double-strand breaks are thought to be repaired primarily by the error-prone non-homologous end-joining pathway, which might result in an accumulation of genomic rearrangements (Mohrin et al., 2010). Interestingly, HSPCs harbor DNA-damage-induced cell-cycle checkpoints and DNA repair mechanisms that differ from those usually found in differentiated tissues and cell lines in terms of activation, outcome, and efficiency. For example, HSCs and less primitive progenitors lack a proper G1/S checkpoint, which results in an inability of these cells to arrest at the G1/S boundary upon DNA damage (Moehrle et al., 2015). Furthermore, human HSPCs lack a decatenation checkpoint, which is usually responsible for the resolution of entangled chromosomes (Damelin et al., 2005). Another crucial checkpoint ensuring genome integrity in somatic tissue is the spindle assembly checkpoint (SAC). The SAC forces an arrest at prometaphase until all chromosomes are correctly aligned to the mitotic spindle (Musacchio and Salmon, 2007). It is thought to be an essential pathway to prevent translocations and aneuploidy, two hallmarks of cancer. There are some indications that hematopoietic progenitor cells arrest in G2/M phase when treated with the spindle drug nocodazole (Rohrabaugh et al., 2008). Furthermore, a recent study showed that fetal HSCs isolated from mice with trisomy (a known consequence of an abrogated SAC) display severe engraftment deficits. Similar problems occurred upon serial transplantation of bone marrow (BM) cells hypomorphic for the SAC component *BubR1* (Pfau et al., 2016). In addition, a recent report demonstrated the requirement of the SAC for satellite cells, suggesting a general relevance of this mechanism for adult stem cells (Kollu et al., 2015). Strikingly, multiple studies report a SAC malfunction in leukemic cells that is linked to the accumulation of translocations and aneuploidies. Leukemia is frequently driven by transformed HSPCs (Schnerch et al., 2013). Given the important role of the SAC for the genetic integrity of somatic tissues and the implications of checkpoint failure in leukemia, it is somewhat surprising that it is actually not known in detail whether the SAC is actually active in HSPCs, and if so, whether it differs

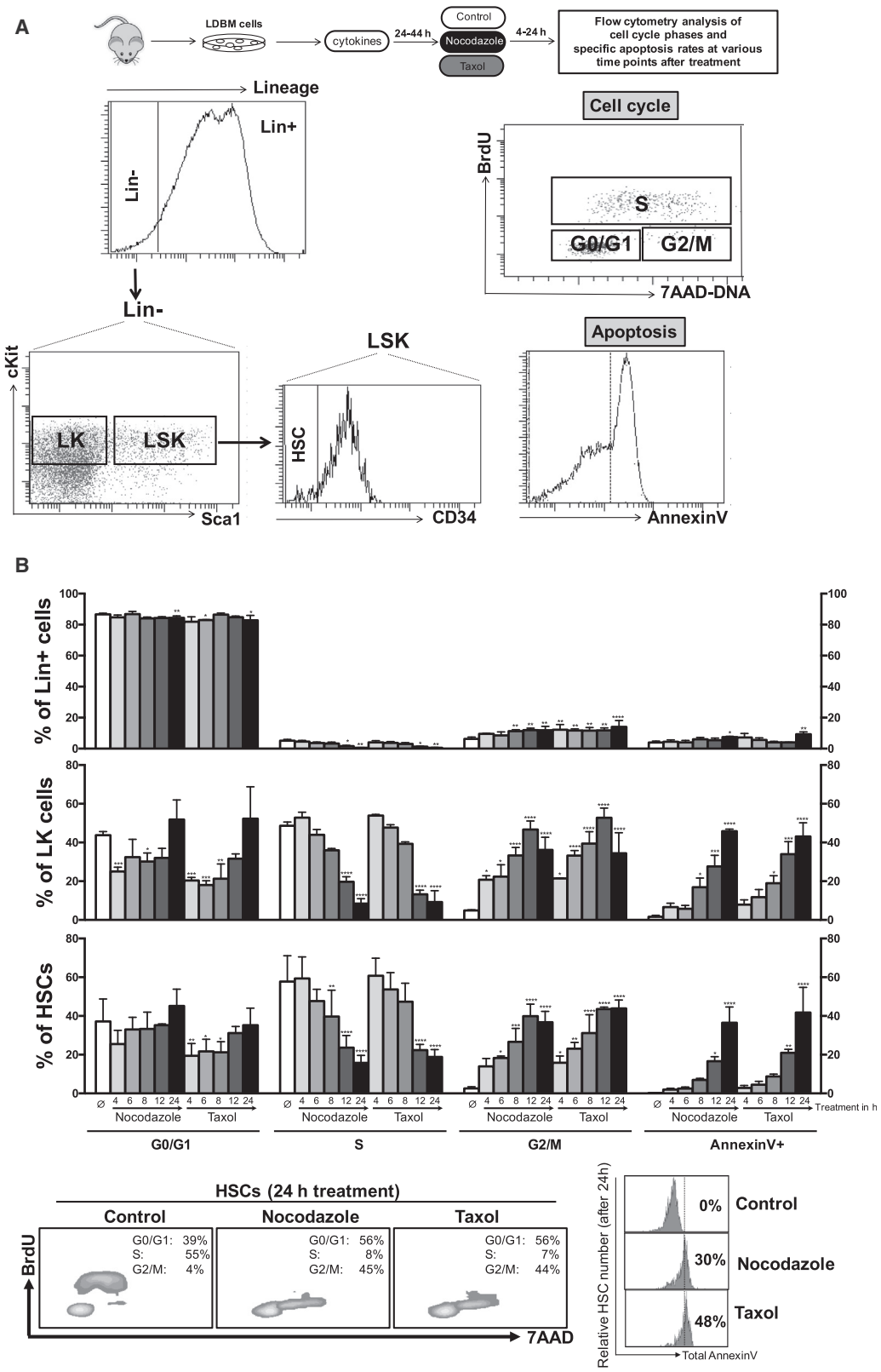

(legend on next page)

mechanistically from the SAC in differentiated tissue and how it might contribute to genomic stability and regulation of hematopoiesis.

RESULTS

Inhibition of Proper Spindle Assembly Induces a G2/M Arrest and p53-Dependent Apoptosis in HSPCs

Prolonged treatment of proliferating somatic cells with anti-mitotic drugs induces a G2/M arrest by activation of the SAC followed by the induction of apoptosis via p53-dependent and -independent mechanisms (Bacus et al., 2001; Zhang et al., 2002). To determine the mitotic checkpoint response in HSPCs, low-density bone marrow (LDBM) cells, containing HSPCs and differentiated cells isolated from C57BL/6 mice were incubated with cytokines to allow for their activation and entry into the cell cycle. They were subsequently treated with the spindle toxins nocodazole, taxol or, as a control, the solvent DMSO. Cell-cycle position, progression, and apoptosis of distinct types of HSPCs as well as more differentiated cells was determined by flow cytometry at various time points post drug induction. After treatment with cytokines alone (control), HSPCs and especially HSCs were predominantly detected in S phase. When treated with cytokines in conjunction with spindle drugs, HSPCs arrested at the G2/M boundary, whereas their S-phase content was strongly reduced. This effect was observed in lineage-negative cells (Lin−), Lin-cKit+ (LKs), Lin-Sca1+cKit+ cells (LSKs or early progenitor cells), and HSCs but in a slight manner also in differentiated hematopoietic cells (Lin+). Whereas a strong G2/M arrest could be observed shortly after treatment with spindle drugs (4 hr), especially in HSPCs, elevated apoptosis did not appear before 24 hr of treatment. Furthermore, the more primitive HSPC subpopulations (HSCs and LSKs) showed a higher percentage of cells undergoing apoptosis compared with differentiated cells, implying an elevated sensitivity of these types of cells to spindle drugs. High levels of apoptosis were also detected in cells in S phase in all of the analyzed cell populations, but not before 24 hr (Figures 1B, S1A, and S1B). Interestingly, differentiated (Lin+) cells were not significantly affected by spindle drug treatment in terms of cell death. This behavior is not linked to their general lower cycling frequency, as exposure to additional cytokines effectively enhanced replication activity but not apoptosis (Figure S1C). As expected, treatment of unstimulated HSPCs solely with spindle drugs did not induce apoptosis, indicating that quiescent and non-cycling cells do not depend on microtubule dynamics (Figure S2A). We conclude that cycling HSPCs activate G2/M arrest in response to mitotic spindle failure. The data also reveal that apoptosis is only initiated upon prolonged treatment with spindle drugs and thus long-term (24 hr) activation of the checkpoint.

We next tested whether apoptosis upon mitotic arrest of HSPCs is p53-dependent. LDBM cells were again arrested at the G2/M boundary for 24 hr. Indeed, a significant reduction of apoptosis in all distinct HSPC subpopulations derived from *p53* KO mice could be detected compared with wild-type (WT) cells when applying nocodazole. The observed reduction was even higher in response to taxol (Figure S2B). Apoptosis in response to prolonged mitotic arrest of HSPCs is thus, at least in part, p53-dependent.

The Mitotic Checkpoint Is Functionally Active in HSPCs

Upon activation of the SAC, many checkpoint kinases are active, such as Aurora B and MPS1. To further assess the functionality of the SAC in HSPCs, LDBM cells were driven into the cell cycle following a short exposure to taxol. Meanwhile, Aurora B or MPS1 kinases were inhibited by ZM447439 or reversine, respectively. In addition, some of these cells were also exposed to the proteasome inhibitor MG132 for 2 hr. As proteolysis is essential for triggering anaphase onset, MG132-treated cells should arrest even when the checkpoint is inactive. For mitotically arrested cells, phosphorylation of serine 10 or 28 in histone H3 (pH3) was assessed. In cells treated with taxol, a strong arrest in prometaphase could be observed, especially in LSKs and HSCs as judged by high rates of pH3 distribution. Treatment with taxol together with ZM447439 or reversine triggers loss of pH3 signaling, indicating checkpoint override and premature mitotic exit (Figures 2A, 2B, and S3A). Based on the chromatin shape of HSCs, the DNA of taxol and reversine/ZM447439-treated HSCs predominantly appeared decondensed, unlike cells treated only with taxol,

Figure 1. Treatment of HSPCs with Spindle Drugs Arrests Cells at the G2/M Boundary and Induces Apoptosis

(A) Schematic overview of the experiment. LDBM cells were treated with cytokines to induce cell cycling along with nocodazole, taxol, or the corresponding solvent, DMSO (control) for various time points. BrdU was added to the cells 30 min before harvesting following procession for flow-cytometric analysis.

(B) Upper panels: The cell-cycle distribution and the rate of early apoptosis (Annexin V-positive staining) of the indicated LDBM subpopulations were measured. Lower panels: Representative fluorescence-activated cell sorting (FACS) histograms of cell-cycle distribution and Annexin V intensities in HSCs. n = 3. Error bars are SEM with significances tagged with asterisks. *p < 0.05, **p < 0.01, ***p < 0.001, ****p < 0.0001.

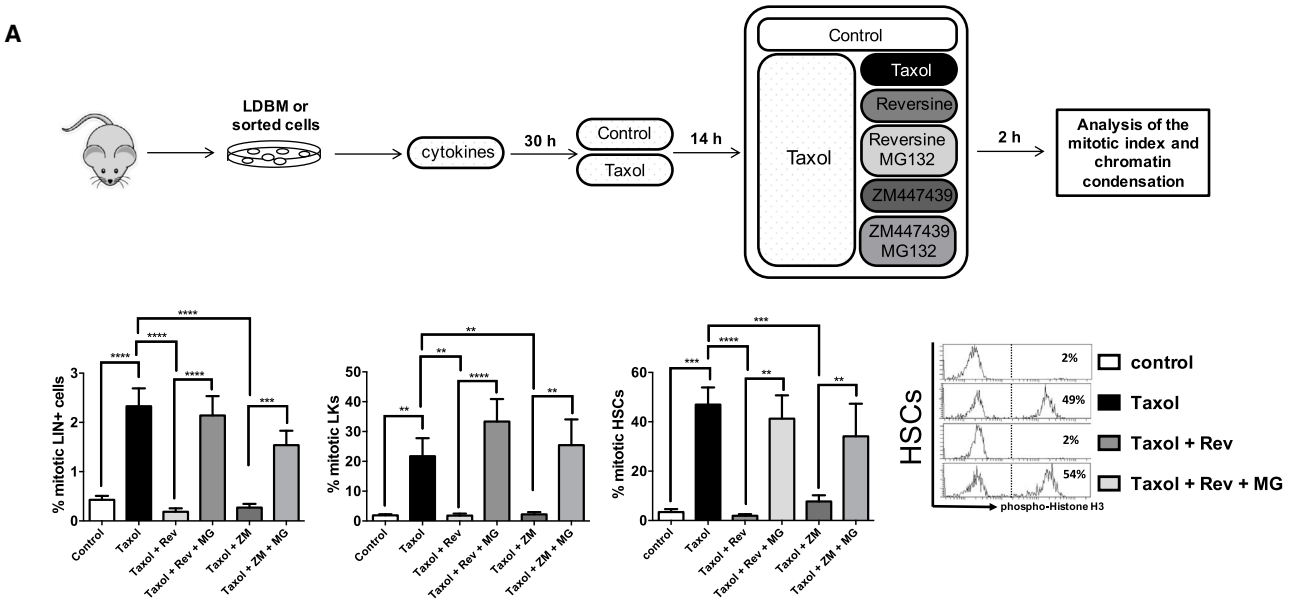

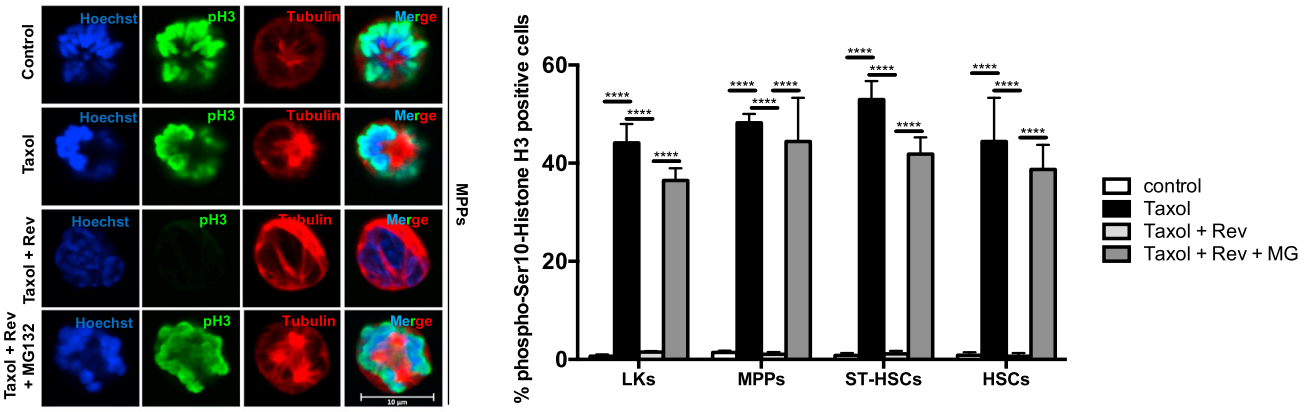

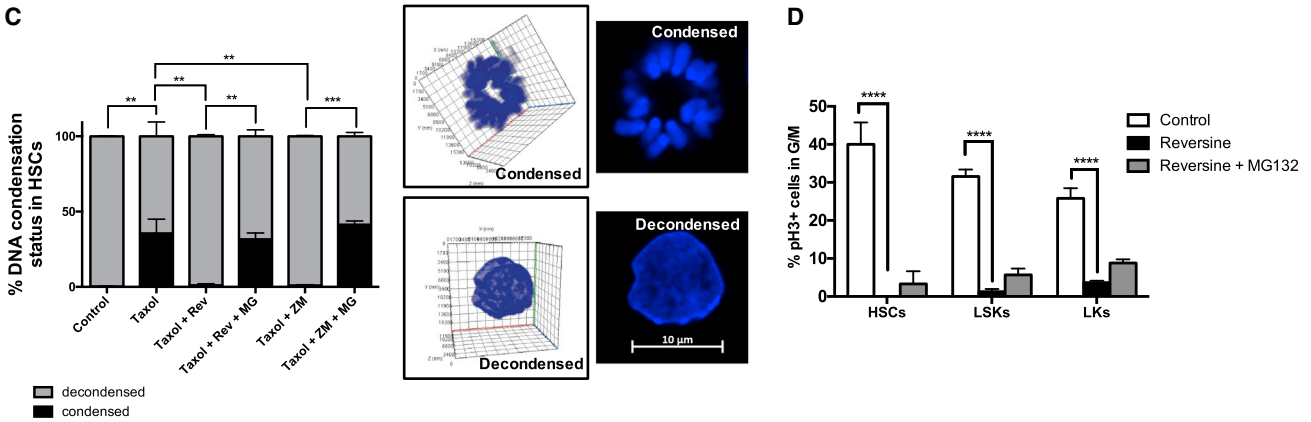

(legend on next page)

harboring predominantly condensed nuclei (Figure 2C, Movies S1 and S2). This mitotic exit in taxol/reversine/ZM447439-treated HSPCs was suppressed by MG132, and cells remained pH3 positive and chromatin condensed, indicating an SAC override with the inability to initiate anaphase, as the function of the proteasome is necessary for chromosome segregation (Figures 2A–2C and S3A). When treating cycling HSPCs solely with reversine, a strong checkpoint inhibition was observed as indicated by the reduced proportion of pH3 within the corresponding G2/M subpopulations. Furthermore, upon simultaneous treatment of these cells with reversine and MG132, a partial rescue of pH3 signaling could be seen (Figure 2D). To exclude that our inhibitors induce pH3 loss due to enhanced rates of apoptosis, HSPCs were treated as indicated and stained against the active (cleaved) form of caspase-3. Indeed, no significant or only moderate activation of caspase-3 could be observed (Figure S3B). Interestingly, when HSCs were treated with a combination of taxol and reversine, signs of re-initiation of DNA synthesis likely linked to tetraploidy could be observed based on 5-bromo-2-deoxyuridine (BrdU)/7AAD staining. As expected, especially P53-deficient HSCs presented with such a re-initiation of DNA synthesis. This effect was absent in LK cells, independent of the p53 status (Figure S3C). We also investigated the SAC in NIH/3T3 fibroblasts as a positive control. As anticipated, fibroblasts present with an active SAC. Upon treatment with various SAC inhibitors, we also observed minor signs of polyploidy (Figures S3D–S3G). Together, these data demonstrate that HSPCs as well as NIH/3T3 cells are able to mount a functional SAC.

Spindle Checkpoint Proteins Localize at Kinetochores

We next addressed the question whether the activation of the SAC in HSPCs correlates with the distribution of important checkpoint proteins to centromeres and kinetochores. The kinetochores are important catalyzing centers. Here, the mitotic checkpoint complex is formed, preventing anaphase progression (Musacchio and Salmon, 2007). Some of the key SAC proteins are the Aurora kinases, which are distributed to the kinetochores and centromeres as a response to their phosphorylation upon activation (Vigneron et al., 2004). HSPCs show high levels of phosphorylated Aurora at kinetochores upon treatment with spindle drugs in all cell populations analyzed, while this phosphorylation is almost absent in cells exposed to Ro3306, a CDK1 inhibitor that prevents mitotic entry (Figure 3A). Other critical SAC proteins are BUBR1 and BUB1 (Musacchio and Salmon, 2007). As expected, they both co-localize with active Aurora kinases in HSCs, LSKs, and less primitive progenitors during mitotic arrest, indicating proper activation of these proteins and appropriate SAC activity (Figure 3B).

A Proper Mitotic Checkpoint Is Required for Hematopoiesis

We next determined the consequences of a dis-functional SAC for hematopoiesis. As shown previously, downregulation of the SAC impairs the function of satellite cells and myoblasts, implying that a proper checkpoint is of general importance for adult stem cells (Kollu et al., 2015). In order to test the role of impaired SAC activation in hematopoiesis, HSPCs were driven into the active cell cycle followed by addition of reversine or DMSO. After 24 hr of incubation, cells were used for the colony formation (CFU) assay to assess their differentiation ability. Indeed, SAC inhibition triggered a strong decrease in CFU frequency of HSPCs, with only few small colonies remaining upon reversine treatment (Figure 4A). Furthermore, reversine-treated donor cells showed a decreased engraftment ability at 4 weeks after transplantation, implying impaired function of HSPCs (Figure 4B). However, 12 weeks post transplant, both populations (treated and untreated) contributed similarly to chimerism. These data indicate that activation of

Figure 2. The Mitotic Checkpoint Is Functionally Active in HSPCs

(A) Upper panel: Schematic overview of the experiment. LDBM cells were treated with cytokines for 30 hr followed by control or taxol treatment for 14 hr to induce prometaphase arrest. Thereafter, cells were co-cultured with the Aurora inhibitor ZM447439 or the MPS1 inhibitor reversine alone or in conjunction with the proteasome inhibitor MG132 for a total of 2 hr. Cells were fixed and their mitotic index based on pH3 was determined by flow cytometry. Middle panels: Quantification of the mitotic index in the indicated subpopulations. Right panels: Representative histograms of pH3 in HSCs. n = 5. $^{**}p < 0.01$, $^{***}p < 0.001$, $^{****}p < 0.0001$.

(B) FACS-sorted HSPCs were treated as in (A) and then analyzed by immunofluorescence (IF) using markers directed against pH3 and Tubulin. Left panels show representative images, right panels show the corresponding quantification of pH3 abundance in the indicated subpopulations. DNA was counterstained with Hoechst 33342. 30–100 cells were counted per sample. $^{****}p < 0.0001$.

(C) The percentage of condensed and not condensed HSCs as judged by Hoechst 33342 staining was determined. Left panel: Quantification. Right panel: Representative images. n = 3–4, 30–100 cells per sample were counted. $^{**}p < 0.01$, $^{***}p < 0.001$.

(D) LDBM cells were forced to proliferate following control or reversine treatment for 24 hr. One reversine-treated sample was additionally incubated with MG132 for the last 4 hr and finally BrdU was added to all samples for 30 min. After harvesting, cells were processed for flow cytometry. Along with the different HSPC subpopulations, the pH3 distribution within the G2/M subfractions was analyzed. n = 3. $^{****}p < 0.0001$.

Error bars are SEM with significances tagged with asterisks.

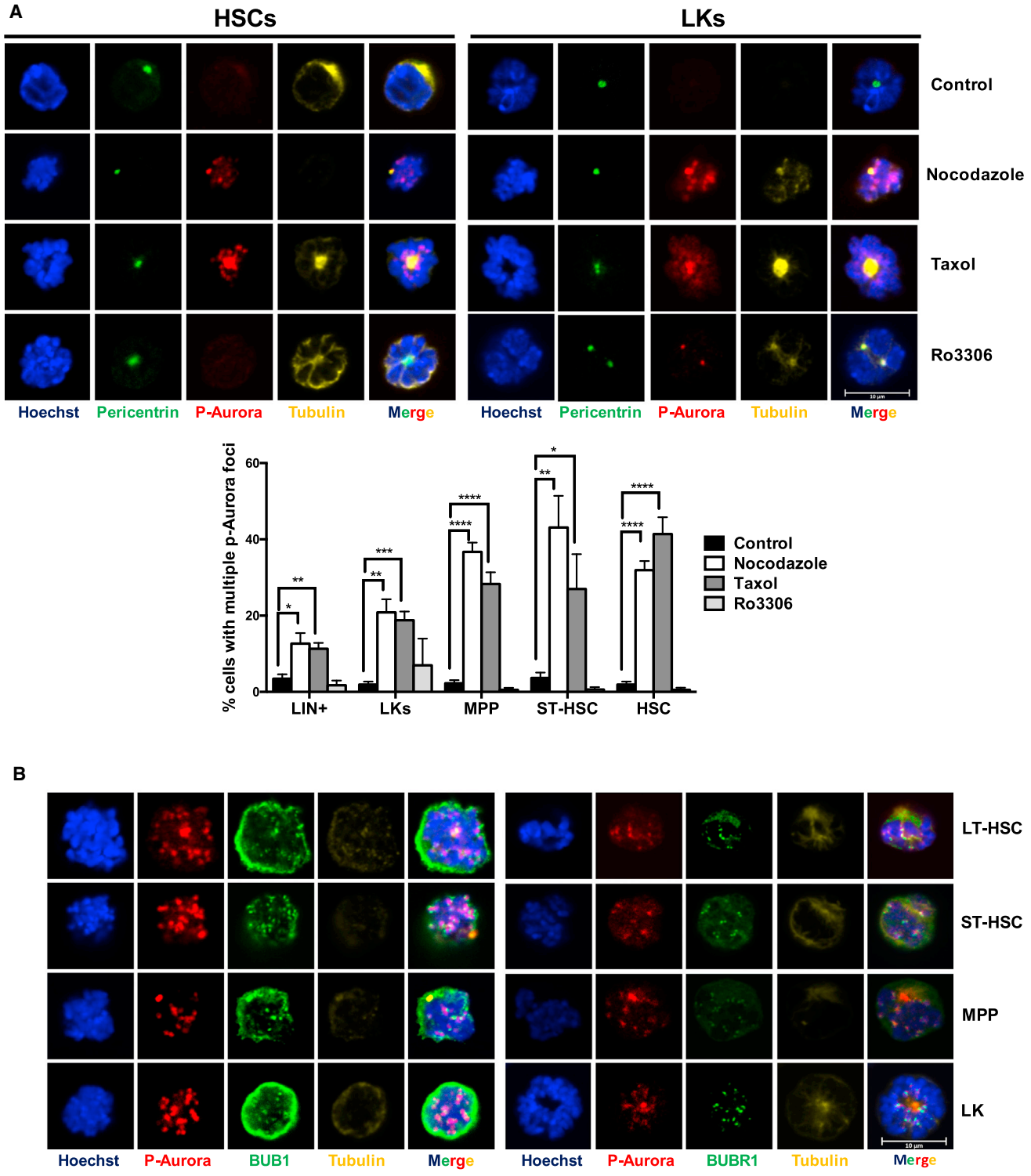

Figure 3. Treatment of HSPCs with Spindle Toxins Triggers the Distribution of Checkpoint Proteins to the Kinetochores

(A) FACS-sorted BM cells (Lin+, LKs, MPPs, ST-HSCs, and HSCs) were induced to enter the cell cycle by cytokines followed by a 24 hr treatment with the spindle toxins nocodazole/taxol or with the CDK1 inhibitor Ro-3306. Following fixation, cells were stained using antibodies directed against phospho-Aurora kinases and Centrin-2. Upper panels: Representative IF images. Bottom panel:

(legend continued on next page)

the SAC primarily impairs the proliferation of hematopoietic progenitors but less the function of HSCs, as early phases of engraftment mostly depend on committed progenitors, whereas engraftment at later time points is driven by more primitive cells (Busch et al., 2015). Furthermore, no difference in the percentage of myeloid or lymphoid lineages in peripheral blood was observed, indicating that the differentiation potential of HSCs was not affected by the SAC inhibition (Figure S4A). Importantly, apoptosis can be excluded as a contributor to the observed impaired engraftment (Figure S4B). However, reversine induced a strong G0/G1 arrest in HSPCs (Figures 4C and S4C). A similar arrest was observed previously in satellite cells when genetically inhibiting the target of reversine, Mps1 (Kollu et al., 2015). These results thus indicate that HSPCs harbor a safety mechanism arresting post-mitotic cells with a corrupted SAC in order to prevent potentially damaged cells from further cycling. Moreover, when treating cycling HSPCs as well as NIH/3T3 fibroblasts with reversine in conjunction with cytochalasin D to prevent cytokinesis, enhanced levels of chromosomal damage were observed, especially in fibroblasts and more committed progenitors but less in HSCs (Figure 4D). These data demonstrate that SAC abrogation indeed induces chromosomal damage, although mostly affecting less primitive BM cells and not HSCs directly.

Expression of the SAC component BubR1 has been shown to be downregulated in BM cells in patients with acute myeloid leukemia, causing reduced SAC activity and decreased sensitivity to spindle drugs (Schnerch et al., 2013). In addition, *BubR1* hypomorphic BM cells present with an impaired engraftment ability upon serial transplantation (Pfau et al., 2016). We tested the consequences of BubR1 deficiency on HSPC cell-cycle dynamics and hematopoiesis. In LDBM cells from *BubR1* heterozygous mice (*BubR1*$^{-/-}$ animals are embryonic lethal and die of apoptosis; Wang et al., 2004) we observe reduced BUBR1 protein expression (Figure S4D). Cycling HSPCs from these mice, when treated with taxol, resulted in a decrease in pH3 distribution compared with WT cells, particularly in HSCs and LSKs (Figures 4E and S4E). We conclude that HSPCs with only one *BubR1* allele are not able to fully activate the SAC upon exposure to spindle drugs. However, cycling HSPCs treated correspondingly with DMSO or taxol isolated from WT or *BubR1*$^{+/-}$ mice did not show any significant differences in the number of CFUs (granulocyte-macrophage progenitors) as well as CFU-E (erythroid progenitors) colonies, indicating that one *BubR1* allele may still be capable of sustaining normal hematopoiesis with a partially active SAC (Figure S4F). Similarly, the absolute numbers in BM and cell-cycle characteristics of various progenitors, such as common lymphoid progenitors, LKs, and LSKs, but also HSCs obtained from BubR1$^{+/-}$ mice, were similar compared with those for WT mice, indicating that partial loss of *BubR1* affects hematopoiesis only to a small extent, as only LKs presented with a trend toward being more in S phase (Figures 4F and 4G). In addition, activated *BubR1*$^{+/-}$ HSPCs do not exhibit enhanced levels of chromosomal aberrations after cell division compared with WT cells (Figure S4G).

In summary, the mitotic checkpoint is active in HSPCs but might be only partially dependent on BubR1. A dysfunctional checkpoint affects primarily the function of progenitor cells but not more primitive types of cells such as HSCs directly.

DISCUSSION

Here, we demonstrate that murine HSCs and hematopoietic progenitors harbor a functional mitotic checkpoint. Actively cycling HSPCs in general and especially HSCs arrest at prometaphase when treated with spindle toxins followed by the induction of cell death after prolonged (24 hr) treatment with the drug. The SAC can be abrogated by inhibiting some of its key components, such as MPS1 and Aurora B, leading to premature mitotic exit and chromosomal abnormalities. We furthermore show that by inhibiting the checkpoint in proliferating HSPCs, hematopoiesis is partially corrupted as judged by decreased colony formation ability and impaired engraftment. HSPCs with only one *BubR1* allele fail to sufficiently arrest at mitosis when exposed to taxol. Importantly, HSPCs from *P53* KO mice do not exhibit high levels of apoptosis after extended treatment with spindle drugs. This finding is consistent with a loss of p53 as a critical driver of leukemogenesis (Wong et al., 2015). However, anti-mitotic drugs also induce apoptosis in other cell-cycle phases besides G2/M in HSPCs. After prolonged treatment (24 hr), severe apoptosis was detected in S phase as well. Without the addition of cytokines, apoptosis was barely detectable. These observations could indicate that spindle drugs have side effects especially on cycling HSPCs, which warrant further investigation.

How does the SAC contribute to the maintenance of the HSPC pool to enable proper function of HSPCs and to

quantifications. n = 3; 30–100 cells per sample were counted. Error bars are SEM with significances tagged with asterisks. *p < 0.05, **p < 0.01, ***p < 0.001, ****p < 0.0001.

(B) Similar to (A), sorted and taxol-treated cells (8 hr) of the indicated subpopulations were stained with antibodies targeted against BUBR1, BUB1, p-Aurora kinases, and Tubulin. DNA was counterstained with Hoechst 33342.

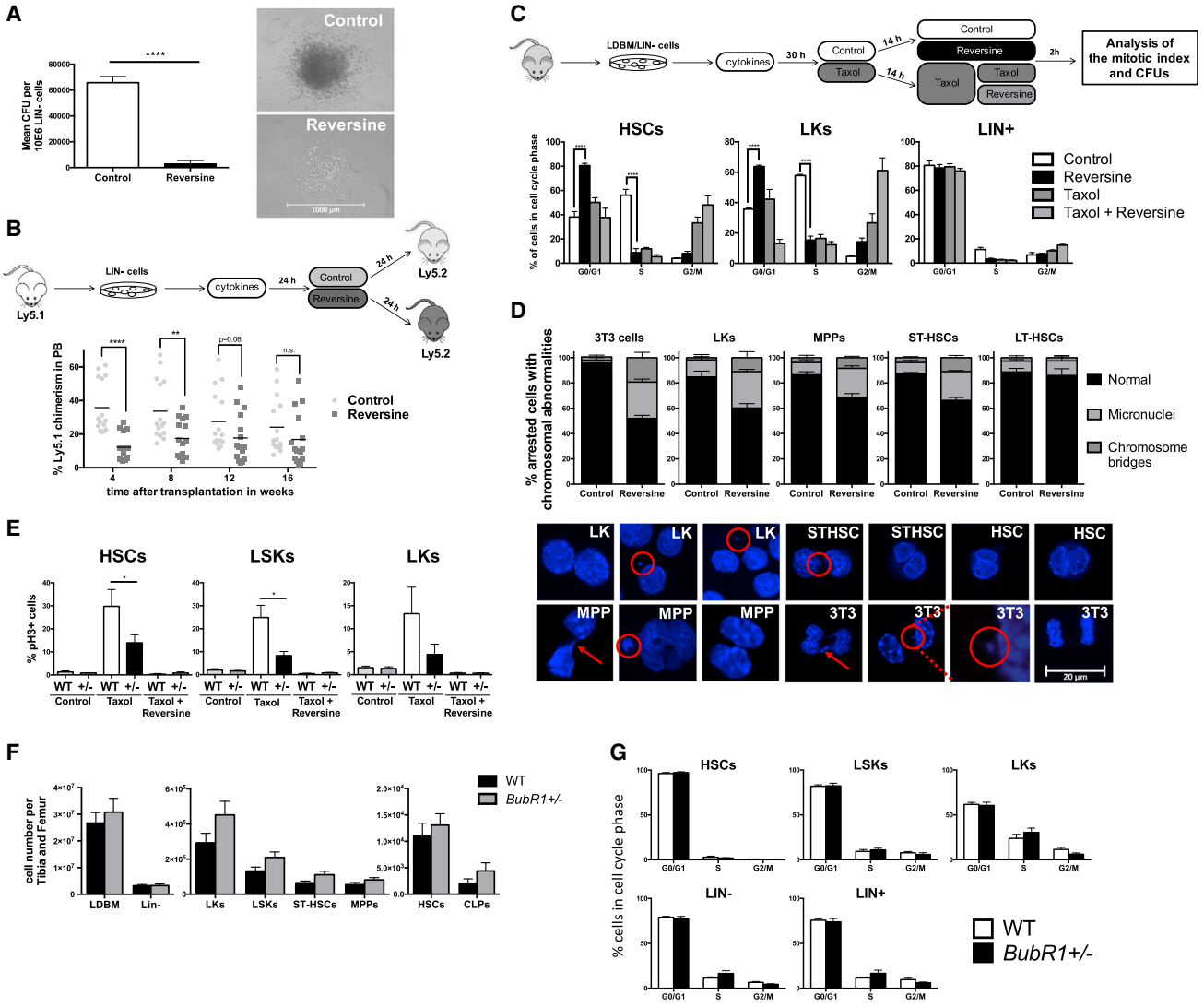

Figure 4. The SAC Is Required for Hematopoiesis

(A) Lin− cells obtained from WT mice were driven into the cell cycle with cytokines following 24 hr control or reversine treatment and procession for the CFU assay. Left panel: Quantification. Right panel: Representative images. n = 3. ****p < 0.0001.

(B) Left panel: Schematic overview of the experiment. Cytokine-treated Lin− cells from donor Ly5.1 mice were treated with reversine or DMSO following transplantation into lethally irradiated recipients (Ly5.2) and regular analysis of Ly5.2/Ly5.1 chimerism in PB by flow cytometry. Right panel: Quantification. n = 3, 5 mice per group, 30 mice in total. **p < 0.01, ****p < 0.0001.

(C) Top panel: Schematic overview of the experiment. LDBM cells were treated with cytokines and DMSO, reversine, taxol, or a combination of the last two compounds. Cells were labeled with BrdU 30 min before harvesting. Thereafter, cells were analyzed in terms of cell-cycle phases and apoptosis. Bottom panel: Quantification. n = 3. ****p < 0.0001.

(D) NIH/3T3 cells as well as cytokine-stimulated HSPCs were treated with reversine or DMSO and cytochalasin D for 12 hr. Thereafter cells were fixed, stained with Hoechst followed by the analysis of chromosome bridges and nuclei in cytokinesis-arrested cells. Left panel: Quantification. Right panels: Representative Hoechst images. Micronuclei or chromosome bridges are indicated by circles or arrows, respectively. n = 3.

(E) LDBM cells isolated from *BubR1*$^{+/-}$ or WT mice, respectively were treated with cytokines following treatment with taxol or the corresponding control, DMSO for 14 hr. Two hours before harvesting and processing for the analysis of the mitotic index, taxol-treated cells were further incubated with reversine or its control, DMSO. n = 4. *p < 0.05.

(legend continued on next page)

prevent genomic instability and potentially transformation? DNA mutations are believed to be the major driver of HSC exhaustion in old mice (Dykstra et al., 2011). For dormant or quiescent HSCs, a functional SAC would be of no great importance as cells are not cycling and mostly reside in G0. This is supported by our observation that non-cytokine-treated HSPCs do not show enhanced levels of apoptosis upon spindle drug treatment, even those in G2/M phase. Furthermore, *BubR1*$^{+/-}$ HSCs do not show abnormalities in terms of cell-cycle distribution and absolute cell numbers, whereas LKs could be found to be more enriched in S phase and less in G2/M phase, although this difference was not significant. This indicates that, especially for HSCs from adult mice, *BubR1* does not alter cell-cycle dynamics. These observations are supported by recent studies from Pfau et al. (2016). Here, the authors used hypomorphic *BubR1* BM cells for serial transplantation assays. Engraftment defects did not occur before secondary transplantation (Pfau et al., 2016). Interestingly, when cycling HSPCs are treated with the checkpoint inhibitor reversine, chromosomal damage occurs and a durable G0/G1 arrest is induced. This could argue for a post-mitotic safety mechanism preventing checkpoint-abrogated HSPCs from further cycling. A similar pathway was described in satellite cells and, according to the authors, could contribute to genome integrity of stem cells (Kollu et al., 2015). Our data also suggest that a functional SAC is more critical for committed progenitors than for more primitive compartments as indicated in our transplantation experiments. This assumption is supported by low numbers of chromosomal aberrations in HSCs upon reversine treatment. As steady-state hematopoiesis is primarily driven by progenitors and not by HSCs (Busch et al., 2015), a functional SAC might be critical for hematopoiesis. A dysfunctional SAC might thus contribute to BM failure but also, in the long-run, genetic instability in HSPCs.

EXPERIMENTAL PROCEDURES

Mice

C57BL/6 mice 8–16 weeks old were purchased by Janvier. *p53* KO mice were developed previously and kept at the mouse facilities of the University of Ulm. *BubR1* heterozygous mice developed previously were kindly provided by Darren J. Baker (Mayo Clinic, MA) and kept at the mouse facility of Cincinnati Children's Hospital Medical Center (CCHMC). All mouse experiments were performed in compliance with the German Law for Welfare of Laboratory Animals and were approved by the Regierungspräsidium Tübingen or the IACUC at CCHMC.

Cell Culture

For *in vitro* experiments, cells were cultured using IMDM medium supplemented with 1/100 GlutaMax (Gibco) in an incubator with 5% CO_2 at 37°C and normal oxygen conditions. HSCs were cultured using an incubator with 3% oxygen.

Statistical Analysis

Normal distribution of data was implied and the variance between the groups was similar. All statistical analyses were performed using Student's t test or two-way ANOVA when appropriate with GraphPad Prism 6 software. The number of biological repeats for every experiment (n) is mentioned in the figure legends. Error bars are SEM with significances tagged with asterisks: *$p < 0.05$, **$p < 0.01$, ***$p < 0.001$, ****$p < 0.0001$.

For detailed experimental procedures, please see Supplemental Information.

SUPPLEMENTAL INFORMATION

Supplemental Information includes Supplemental Experimental Procedures, four figures, and two movies and can be found with this article online at https://doi.org/10.1016/j.stemcr.2017.09.017.

AUTHOR CONTRIBUTIONS

A.B. designed, conducted, and analyzed most of the experiments with essential support from J.P. and K.E.; D.J.B. supported us with the *BubR1*$^{+/-}$ mouse model; B.M. developed the assay used in Figures 1, 4, S1, S2, and S4; V.S. performed the transplantation; K.N. helped with experiments involving *BubR1*$^{+/-}$ mice; M.V. performed confocal imaging; A.G. contributed to the experiments shown in Figures 4D and S4G. H.G. supervised and interpreted most experiments. H.G. and A.B. wrote the paper.

ACKNOWLEDGMENTS

We thank the FACS core at Ulm University for cell sorting and the Central Animal Facility of Ulm University as well as the Comprehensive Mouse and Cancer Core at CCHMC for help with mouse experiments. We are grateful to Stephan Stilgenbauer and Hans Jörg Fehling for providing *p53* KO mice and Steven Taylor for anti-BUBR1/BUB1 antibodies. We thank the core facility confocal microscopy for providing assistance with imaging. Furthermore, we thank Nicola Martin, Gina Marka, and Karin Soller for technical assistance and all members of the group for discussions. Work in the laboratory of H.G. was supported by the Deutsche Forschungsgemeinschaft SFB 1074 and SFB 1149, the

(F) The indicated BM subpopulations from WT or *BubR1*$^{+/-}$ mice were analyzed by flow cytometry. Relative numbers were calculated as absolute numbers per tibia and femur. n = 3.
(G) Young WT or *BubR1*$^{+/-}$ mice were injected i.p. with 300 μL of 2.5 mg/mL BrdU for 45 min. After scarification, LDBM cells were isolated following staining of surface markers, S phase, and DNA. n = 5.
Error bars are SEM with significances tagged with asterisks.

Excellence-Initiative of the Baden-Württemberg Foundation, the Edward P. Evans Foundation, and the National Institute of Health, AG040118, DK104814, and AG05065. A.B. was supported by a Bausteinprogramm of the Medical Faculty of Ulm University.

Received: February 6, 2017
Revised: September 21, 2017
Accepted: September 22, 2017
Published: October 19, 2017

REFERENCES

Bacus, S.S., Gudkov, A.V., Lowe, M., Lyass, L., Yung, Y., Komarov, A.P., Keyomarsi, K., Yarden, Y., and Seger, R. (2001). Taxol-induced apoptosis depends on MAP kinase pathways (ERK and p38) and is independent of p53. Oncogene *20*, 147–155.

Busch, K., Klapproth, K., Barile, M., Flossdorf, M., Holland-Letz, T., Schlenner, S.M., Reth, M., Höfer, T., and Rodewald, H.R. (2015). Fundamental properties of unperturbed haematopoiesis from stem cells in vivo. Nature *518*, 542–546.

Damelin, M., Sun, Y.E., Sodja, V.B., and Bestor, T.H. (2005). Decatenation checkpoint deficiency in stem and progenitor cells. Cancer Cell *8*, 479–484.

Dykstra, B., Olthof, S., Schreuder, J., Ritsema, M., and de Haan, G. (2011). Clonal analysis reveals multiple functional defects of aged murine hematopoietic stem cells. J. Exp. Med. *208*, 2691–2703.

Holyoake, T., Jiang, X., Eaves, C., and Eaves, A. (1999). Isolation of a highly quiescent subpopulation of primitive leukemic cells in chronic myeloid leukemia. Blood *94*, 2056–2064.

Kollu, S., Abou-Khalil, R., Shen, C., and Brack, A.S. (2015). The spindle assembly checkpoint safeguards genomic integrity of skeletal muscle satellite cells. Stem Cell Reports *4*, 1061–1074.

Moehrle, B.M., Nattamai, K., Brown, A., Florian, M.C., Ryan, M., Vogel, M., Bliederhaeuser, C., Soller, K., Prows, D.R., and Abdollahi, A. (2015). Stem cell-specific mechanisms ensure genomic fidelity within HSCs and upon aging of HSCs. Cell Rep. *13*, 2412–2424.

Mohrin, M., Bourke, E., Alexander, D., Warr, M.R., Barry-Holson, K., Le Beau, M.M., Morrison, C.G., and Passegué, E. (2010). Hematopoietic stem cell quiescence promotes error-prone DNA repair and mutagenesis. Cell Stem Cell *7*, 174–185.

Musacchio, A., and Salmon, E.D. (2007). The spindle-assembly checkpoint in space and time. Nat. Rev. Mol. Cell Biol. *8*, 379–393.

Pfau, S.J., Silberman, R.E., Knouse, K.A., and Amon, A. (2016). Aneuploidy impairs hematopoietic stem cell fitness and is selected against in regenerating tissues in vivo. Genes Dev. *30*, 1395–1408.

Rohrabaugh, S., Mantel, C., and Broxmeyer, H.E. (2008). Mouse hematopoietic stem cells, unlike human and mouse embryonic stem cells, exhibit checkpoint-apoptosis coupling. Stem Cells Dev. *17*, 1017–1020.

Schnerch, D., Schmidts, A., Follo, M., Udi, J., Felthaus, J., Pfeifer, D., Engelhardt, M., and Wäsch, R. (2013). BubR1 is frequently repressed in acute myeloid leukemia and its re-expression sensitizes cells to antimitotic therapy. Haematologica *98*, 1886–1895.

Vigneron, S., Prieto, S., Bernis, C., Labbé, J.C., Castro, A., and Lorca, T. (2004). Kinetochore localization of spindle checkpoint proteins: who controls whom? Mol. Biol. Cell *15*, 4584–4596.

Walter, D., Lier, A., Geiselhart, A., Thalheimer, F.B., Huntscha, S., Sobotta, M.C., Moehrle, B., Brocks, D., Bayindir, I., Kaschutnig, P., et al. (2015). Exit from dormancy provokes DNA-damage-induced attrition in haematopoietic stem cells. Nature *520*, 549–552.

Wang, Q., Liu, T., Fang, Y., Xie, S., Huang, X., Mahmood, R., Ramaswamy, G., Sakamoto, K.M., Darzynkiewicz, Z., Xu, M., et al. (2004). BUBR1 deficiency results in abnormal megakaryopoiesis. Blood *103*, 1278–1285.

Wong, T.N., Ramsingh, G., Young, A.L., Miller, C.A., Touma, W., Welch, J.S., Lamprecht, T.L., Shen, D., Hundal, J., Fulton, R.S., et al. (2015). Role of TP53 mutations in the origin and evolution of therapy-related acute myeloid leukaemia. Nature *518*, 552–555.

Zhang, H., Shi, X., Zhang, Q.-J., Hampong, M., Paddon, H., Wahyuningsih, D., and Pelech, S. (2002). Nocodazole-induced p53-dependent c-Jun N-terminal kinase activation reduces apoptosis in human colon carcinoma HCT116 cells. J. Biol. Chem. *277*, 43648–43658.